J. Astrophys. Astr. (2018) 39:16
https://doi.org/10.1007/s12036-017-9497-y

Thermonuclear X-ray burst of MXB 1658-298 with *NuSTAR*

RAHUL SHARMA[1,*], ABDUL JALEEL[1], CHETANA JAIN[2], BISWAJIT PAUL[3] and ANJAN DUTTA[1]

[1]Department of Physics and Astrophysics, University of Delhi, Delhi 110 007, India.
[2]Hansraj College, University of Delhi, Delhi 110 007, India.
[3]Raman Research Institute, Sadashivanagar, C. V. Raman Avenue, Bangalore 560 080, India.
*Corresponding author. E-mail: rahul1607kumar@gmail.com

MS received 28 August 2017; accepted 17 November 2017; published online 10 February 2018

Abstract. MXB 1658-298 is a transient Low-Mass X-ray Binary (LMXB), which shows eclipses, dips and bursts in its light curve. This source has undergone three active periods separated by long quiescent phases. The latest phase of enhanced X-ray emission was observed during 2015–2016. We have analysed broadband data from *Swift*/XRT and *NuSTAR* observations carried out in 2015. During *NuSTAR* observation, one thermonuclear X-ray burst took place. The X-ray emission during the burst was brighter by a factor of ~ 200, compared to the pre-burst emission. This work focuses on the spectral analysis of MXB 1658-298 during the persistent and the burst phases using *NuSTAR* observation of 2015. We have also determined the temperature and radius evolution during the burst using the time-resolved spectroscopy. The burst phase shows mild Photospheric Radius Expansion (PRE).

Keywords. Stars: neutron—X-ray: binaries—X-rays: bursts—X-rays: individual (MXB 1658-298).

1. Introduction

MXB 1658-298 is a transient Low-Mass X-ray Binary (LMXB) system which was discovered in 1976 by observations made with SAS-3 (Lewin *et al.* 1976). It has an orbital period of ∼7.1 h and the light curve shows an eclipse lasting for ∼15 min (Cominsky & Wood 1984). About two years after its discovery, MXB 1658-298 went into a quiescent phase for more than 20 years (in't Zand *et al.* 1999). The source was again visible in 1999, during which coherent burst oscillations at a frequency of ∼567 Hz were reported (Wijnands *et al.* 2001). The 0.5–30 keV BeppoSAX spectrum consisted of a combination of soft disk-black body and a harder Comptonized component (Oosterbroek *et al.* 2001). After being X-ray bright for about 2.5 years, the source again went into quiescence close to the beginning of 2001.

Recently, MXB 1658-298 went into another outburst (Bahramian *et al.* 2015; Negoro *et al.* 2015). Interestingly, from observations spanning ∼40 years, measurements of the orbital period have indicated the presence of a circumbinary planet around this binary system (Jain *et al.* 2017). MXB 1658-298 is currently in the quiescent state (Parikh *et al.* 2017).

In an LMXB system, the compact object accretes from a low-mass stellar companion. The accreted matter accumulates on the surface of the compact object, where it is compressed and heated hydrostatically. When the temperature and pressure are high enough, a thermonuclear explosion is triggered. These events (the Type-I X-ray bursts) are observed as a sudden increase in the X-ray luminosity (Lewin *et al.* 1993; Strohmayer & Bildsten 2006). Type-I bursts have been observed in more than 100 low-mass X-ray binaries harboring a neutron star (Liu *et al.* 2007; Galloway *et al.* 2008a). These bursts are excellent tools for the measurement of neutron star parameters (Bhattacharyya 2010).

Time-resolved spectroscopy during thermonuclear bursts have been performed for many sources for the determination of neutron star radius by assuming that the entire surface emits in X-rays (e.g., van Paradijs 1978; Kuulkers *et al.* 2003; Galloway *et al.* 2008a). The background subtracted spectra during these bursts are well modeled by a black body. The persistent emission prior to the burst is generally subtracted as background

(Lewin *et al.* 1993; Bhattacharyya 2010). Photospheric Radius Expansion (PRE) burst where flux reaches the local Eddington limit causing the photosphere to expand above the stellar surface (e.g., Lewin *et al.* 1993), shows a systematic variation in black-body temperature and emission radius. When the photosphere falls back to the neutron star surface, the temperature has the highest value and the black-body radius has the lowest value, which is also called the touchdown (e.g., Kuulkers *et al.* 2003). Time-resolved spectroscopy during the cooling phase after the touchdown is the most widely used method for neutron star radius measurement (e.g., Lewin *et al.* 1993; Özel 2006; Galloway *et al.* 2008a; Güver *et al.* 2012a, b; Güver & Özel 2013).

We have used *Swift*/XRT and *NuSTAR* data for the broadband spectral analysis of MXB 1658-298 during the persistent phase (after removing the bursts, dips and eclipses). During *NuSTAR* observation, one type-I thermonuclear X-ray burst was observed. We have estimated the temperature evolution during the X-ray burst using the standard technique of time-resolved spectroscopy.

2. Observations and data analysis

The Nuclear Spectroscopic Telescope ARray (*NuSTAR*; Harrison *et al.* 2013) consists of two imaging telescopes, which focus 3–79 keV X-rays onto two identical focal planes (usually called focal plane modules A and B, or FPMA and FPMB). MXB 1658-298 was observed with the *NuSTAR* on 28th September 2015 (obsId = 90101013002), for a total exposure time of 51 ks (Table 1). For this work, we have used the most recent *NuSTAR* analysis software distributed with HEASOFT version 6.20 and the latest calibration files (version 20170120) for reduction and analysis of the data. The calibrated and screened event files were generated using the NUPIPELINE. A circular region of radius 100″ centered at the source position was used to extract the source light curve and spectrum. Background light curve and spectrum were extracted from the same region, away from the source. The task NUPRODUCT was used to generate the spectra and response files. The spectra were grouped to give a minimum of 25 counts/bin. The light curves were background-corrected using LCMATH. *NuSTAR* detectors have a triggered read-out, similar to proportional counter but unlike CCD, they are not subject to pile-up distortions (Harrison *et al.* 2013).

MXB 1658-298 was also monitored with *Swift* during the recent outburst. We have focused on the observation which was obtained on the same day as that of *NuSTAR* (see Table 1). The *Swift*/XRT data was analysed using standard tools incorporated in HEASOFT version 6.16 and the latest calibration files (version 20160609). Observation 00081770001 was obtained in the photon counting (PC) mode for which pile-up correction had to be done. The pile-up was corrected using standard procedure as given in XRT online thread[1]. We used XSELECT to extract source events from a circular region of radius 100″ and avoiding the central region of radius 10″. The background events were obtained from the outer regions of the CCD from circular region of radius 150″. Exposure maps were used to create ancillary response files with XRTMKARF, to account for hot pixels and bad columns on the CCD. The latest response matrix file was sourced from the calibration data base. The spectra were grouped to give a minimum of 20 counts/bin.

Table 1. Observation log.

Satellite	OBSId	Time	Exposure (ks)	Mode
NuSTAR	90101013002	2015-09-28	51	Science
Swift/XRT	00081770001	2015-09-28	1.3	PC

We have used XSPEC (Arnaud 1996) for the spectral fitting and have modeled the effects of interstellar absorption, using a multiplicative model component *wabs* (in XSPEC). All spectral uncertainties and upper-limits are given at 90% confidence.

3. Results

Figure 1 shows the 3–78 keV *NuSTAR*-FPMA light curve of MXB 1658-298 binned with 0.5 s. The observation spans over 17 satellite orbits. During this observation, one type-I thermonuclear X-ray burst was observed at MJD 57294.941086[2], during which the count rate increased by a factor of more than 200. The persistent phase had an average count rate of ∼3 count/s; and about 700 count/s were recorded during the burst phase. The burst profile is shown in Fig. 2. The burst had a rise time of about 3 s followed by ∼5 s of a flat profile having an average count rate of 500–700 count/s. The burst initially displayed a sharp decay with decay time of ∼2 s between 8–10 s of burst start and then it

[1] http://www.swift.ac.uk/analysis/xrt/pileup.php.

[2] Barycenter corrected.

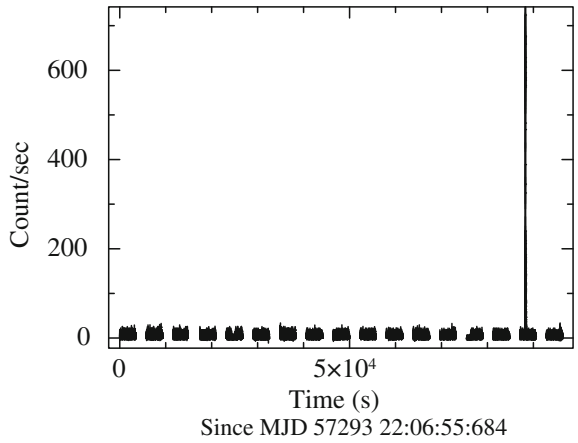

Figure 1. 3–78 keV *NuSTAR*-FPMA light curve of MXB 1658-298 binned with 0.5 s.

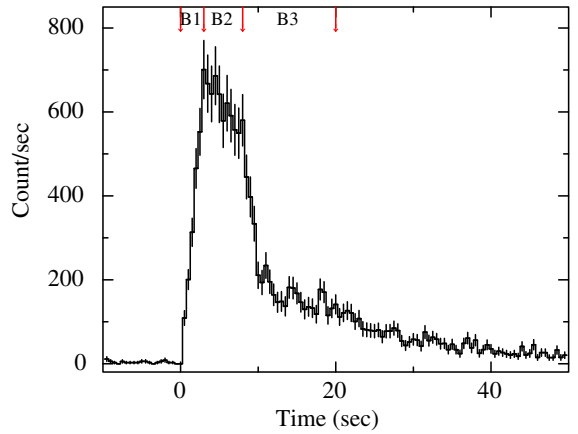

Figure 2. 3–78 keV burst profile of the *NuSTAR* (FPMA) observation binned with 0.5 s. B1, B2 and B3 correspond to different burst phases as described in section 3.2.

decayed exponentially with decay time of 14 s. MXB 1658-298 is known to show a wide spectrum of burst profiles (Wijnands *et al.* 2002).

A comparison of 3–6 keV and 6–30 keV burst profiles and hardness ratio of bursts of MXB 1658-298 is shown in Fig. 3. Burst in soft energies decays faster. Using the assumption that during thermonuclear bursts, neutron star emits like a black-body, the temperature can be inferred from the ratio of the count rates in two energy bands, i.e. hardness ratio (Beri *et al.* 2016). The hardness ratio first decreases, and at around 10 s of burst start to increases again, inferring that there is an increase in temperature around that phase.

3.1 *Persistent emission*

MXB 1658-298 was significantly detected above the background in the entire *Swift*/XRT band (0.4–10 keV)

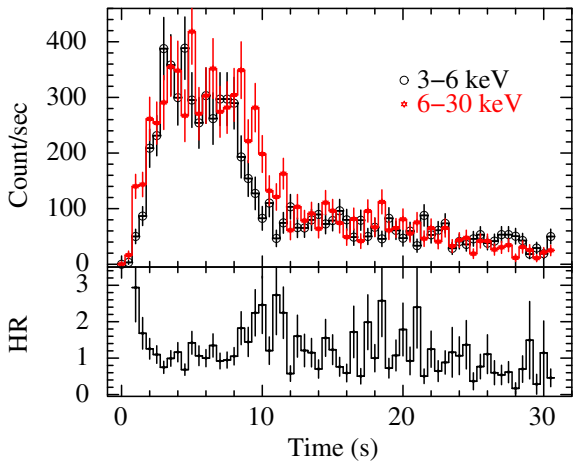

Figure 3. *Top panel*: Burst profile of 2015 *NuSTAR* observation where black (open circle) corresponds to 3–6 keV while red (filled circle) is for 6–30 keV. *Bottom panel*: Hardness ratio between two energy bands.

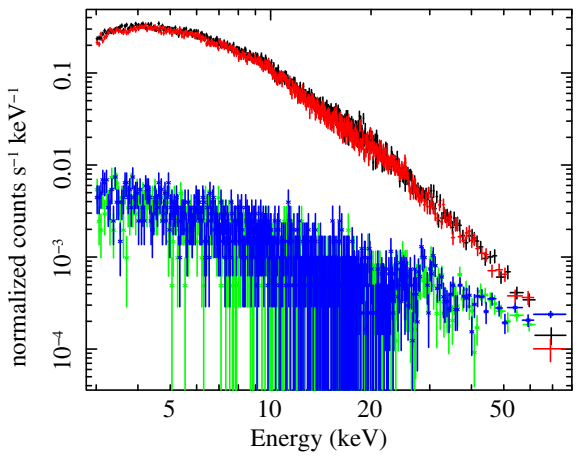

Figure 4. The persistent spectrum of MXB 1658-298 extracted from the *NuSTAR* observations with background. Black and red correspond to source spectra for FPMA and FPMB respectively, and green and blue correspond to background spectra for FPMA and FPMB respectively.

and up to 60 keV in *NuSTAR*. Figure 4 shows the comparison between source and background spectrum obtained from *NuSTAR*. Above 60 keV, the count rate of the source significantly decreases to the background level. So for *NuSTAR*, we have restricted our spectral analysis up to 60 keV only. Figure 5 shows the 0.4–60 keV spectrum of the persistent region of *Swift*/XRT, *NuSTAR*-FPMA and *NuSTAR*-FPMB modeled together. A constant factor was added to account for the cross-calibration of different instruments. The value of the constant for *NuSTAR*-FPMA was fixed to 1 and was kept as a free parameter while fitting the spectrum of the

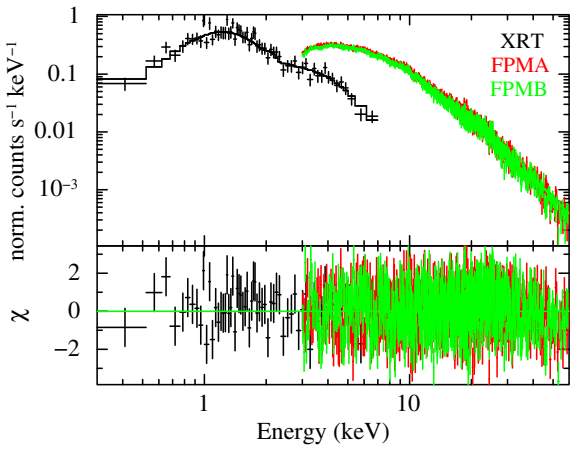

Figure 5. The persistent spectrum of MXB 1658-298 extracted from the *NuSTAR* and *Swift*/XRT observations. It was modeled with absorbed black body and power law.

Table 2. Best-fit spectral parameters of MXB 1658-298 for *NuSTAR* and *Swift*/XRT observation.

Model	Component	Parameters
Constant	C_{XRT}	1.10 ± 0.06
	C_{FPMA}	1.0^{fixed}
	C_{FPMB}	1.015 ± 0.007
wabs	N_H (10^{22} cm^{-2})	0.27 ± 0.03
bbodyrad	kT_{bb} (keV)	1.01 ± 0.05
	Norm	$0.77 \pm^{0.19}_{0.17}$
Power law	Γ	1.79 ± 0.02
	Norm ($\times 10^{-2}$ photons/keV/cm^2/s)	2.1 ± 0.1
	†Flux$_{3-20}$	1.015 ± 0.005
	†Flux$_{0.5-60}$	2.04 ± 0.01
	χ^2/dof	1429/1348

†Unabsorbed flux in units of 10^{-10} erg cm^{-2} s^{-1}.

other two data. The broadband spectra of MXB 1658-298 were fitted with a model consisting of absorbed black-body and power-law and the best-fit parameters are black-body temperature of 1.01 ± 0.05 keV, photon index of 1.79 ± 0.02 and equivalent hydrogen column density of $N_H = (2.7 \pm 0.3) \times 10^{21}$ cm^{-2} (see Table 2). The best fit had a reduced χ^2 of 1.06 for 1348 d.o.f. These results are in coherence with the earlier known results from previous outbursts (Oosterbroek *et al.* 2001; Sidoli *et al.* 2001; Díaz Trigo *et al.* 2006).

3.2 *Burst spectra*

We divided the burst into three parts: burst rise, burst top and burst decay (see Fig. 2). We extracted the burst

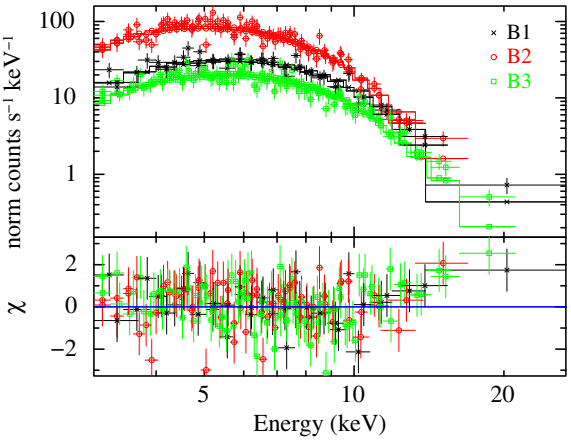

Figure 6. *Top panel*: Burst spectrum of MXB 1658-298 during the three phases (B1, B2 and B3) as described in the text. *Bottom panel*: Residues between data and model.

Table 3. Spectral parameters of burst phases.

Parameters	B1	B2	B3
kT_{bb} (keV)	1.97 ± 0.10	1.61 ± 0.05	1.93 ± 0.07
Radius (km)	$7.7^{+0.9}_{-0.7}$	$17.4^{+1.2}_{-1.1}$	$6.4^{+0.5}_{-0.4}$
†Flux$_{3-20\ keV}$	8.6 ± 0.5	18.7 ± 0.7	5.5 ± 0.2
χ^2_{red}/dof		1.04/210	

†Unabsorbed flux in units of 10^{-9} erg cm^{-2} s^{-1}.

spectrum from these three parts B1 (= 0–3 s; rise), B2 (=3–8 s; top) and B3 (= 8–20 s; decay). We used the standard technique to analyse the burst using persistent spectra as background (Galloway *et al.* 2008a). Spectra extracted from 4.1 ks observation before burst (i.e. of persistent region) was used as background. We fitted all the three spectra of B1, B2 and B3 phase together. We removed the constant of calibration between FPMA and FPMB, as the persistent spectra obtained with the two individual detectors showed good agreement. The three spectra were fitted with an absorbed black-body (wabs $\times$ bbodyrad) with $\chi^2_{red} = 1.04$ for 210 d.o.f (Fig. 6). The black-body temperatures (kT) were 1.97 ± 0.10 keV, 1.61 ± 0.05 keV and 1.93 ± 0.07 keV for B1, B2 and B3 respectively (Table 3). N_H is fixed to 2.7×10^{21} cm^{-2} for all the analysis unless specified.

The time-resolved spectroscopy of the burst (Fig. 7) shows mild Photospheric Radius Expansion (PRE) burst phase suggesting that the flux has reached the Eddington limit. The burst peak bolometric flux was $(2.3 \pm 0.1) \times 10^{-8}$ erg cm^{-2} s^{-1}. The distance measured from peak bolometric flux assuming it did not exceed the Eddington limit for helium burst is $\sim$10 kpc which is in agreement with Muno *et al.* (2001). For

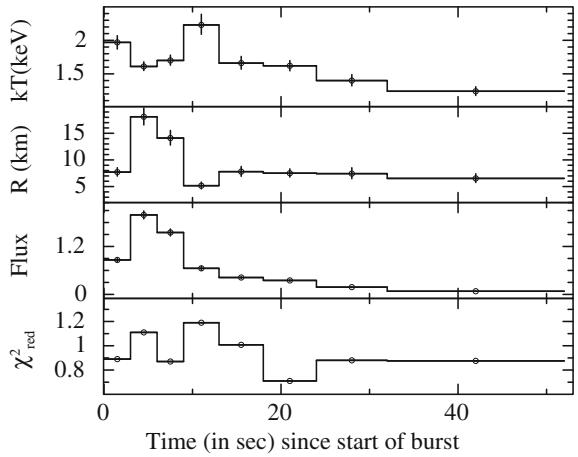

Figure 7. The time-resolved spectroscopy of X-ray burst of MXB 1658-298. *Panel* 1: Black-body temperature, *panel* 2: emission radius calculated from normalization of black body using distance of 10 kpc, *panel* 3: 3–20 keV unabsorbed flux in units of 10^{-8} erg cm^{-2} s^{-1}, *panel* 4: reduced χ^2 with black body fit.

calculation of black-body emission radius from the normalization of bbodyrad, we used the distance of 10 kpc. The 3–20 keV unabsorbed flux during persistent region was $\sim 1.01 \times 10^{-10}$ erg cm^{-2} s^{-1} and the flux during the peak of burst reached up to 1.99×10^{-8} erg cm^{-2} s^{-1}, implying that the flux increased by factor of ∼200 during the burst.

During burst decay phase, the black-body temperature rises to $2.23^{+0.16}_{-0.14}$ keV and the black-body radius decreases (see Fig. 7). This is indicative of the touch-down phase where the photosphere settle down on the surface of the neutron star. The black-body radius measured after the touch-down phase is widely used for neutron star radius measurements (e.g., Lewin *et al.* 1993; Galloway *et al.* 2008a).

4. Discussions and conclusion

In this work, we have reported the broadband spectral study of MXB 1658-298 with *Swift*/XRT and *NuSTAR*. The broadband persistent spectrum can be modeled with absorbed black-body and power-law. We have performed the spectral analysis of MXB 1658-298 during the thermonuclear burst observed with *NuSTAR* during 2015. The 3–20 keV peak flux during the burst increased by a factor of nearly 200 compared to the persistent flux. The burst profile consists of a steep rise, a flat top and a sharp decaying phase. We extracted the spectra from these phases and modeled them using the absorbed black body. The black-body temperatures (kT) obtained from the rise, top and decay part of bursts were 1.97 ± 0.10 keV, 1.61 ± 0.05 keV and 1.93 ± 0.07 keV respectively. In MXB 1658-298, the temperature was observed to decrease for the flat-top part of burst, then increased during the decaying part, and the black-body emission radius increased for burst top part and decreased for burst decay. This is suggestive of a mild PRE burst. In the case of extreme PRE bursts, the temperatures decrease significantly, so that the emission even goes outside the X-ray window (towards UV).

We have also performed the time-resolved spectroscopy of burst using the standard technique. The evolution of temperature and radius indicates towards the Photosphere Radius Expansion (PRE). The PRE phase suggests that the emission during the burst reached the Eddington limit, which gives the 10 kpc distance to source (Muno *et al.* 2001); while the persistent emission was weak. A large increase in the burst flux is seen in very few neutron star LMXB systems, such as GRS 1741.9–2853. The ratio of the burst peak bolometric flux to the persistent bolometric flux in this source is reported to be 445, which is amongst the highest observed (Barriére *et al.* 2015).

Our analysis shows that radius expansion phase persists for 4–10 s and the radius increases in ∼4 s, which is a slow increase as compared to the increase in radius in other LMXB systems like 4U 1728-34 (Zhang *et al.* 2016). Nearly after the 10 s of burst start, the black-body temperature rises to $2.23^{+0.16}_{-0.14}$ keV and black-body radius decreases to a minimum, suggesting the touch-down phase where the photosphere settles down on the surface of the neutron star, although the fit in the corresponding bin is not good compared to other bins ($\chi^2_{red} = 1.2$ for 33 dof). However, we still interpret this moment as touchdown. During the touchdown phase, the effective temperature increases beyond 2 keV. It is found that intervals with temperatures greater than ∼2 keV occur during most bursts, suggesting that the radiative flux exceeds the Eddington flux. The small effective areas inferred during high-temperature intervals, indicate that most of the emission during these intervals comes from only a fraction of the stellar surface (Boutloukos *et al.* 2010).

The ratio between peak flux and touch down flux during burst is ∼3.3. Since MXB 1658-298 is a high-inclination source, geometric effects related to obscuration can significantly affect the flux from the stellar surface (Galloway *et al.* 2008b). The high temperatures, low radiative flux and small emitting areas are found during the touch-down phase. Our results are

consistent with the typical characteristics of PRE burst observed in the high-inclined LMXBs.

Acknowledgements

This research has made use of data obtained from the High Energy Astrophysics Science Archive Research Center (HEASARC), provided by NASA-GSFC.

References

Arnaud K. A. 1996, in Jacoby, G. H., Barnes, J., eds, Astronomical Data Analysis Software and Systems V, ASP Conf. Ser. 101, CA, San Francisco: ASP, 17
Bahramian A., Heinke C. O., Wijnands R. 2015, ATel 7957.
Barriére N. M. *et al*. 2015, ApJ, 799, 123
Beri A., Paul B., Orlandini M., Maitra C. 2016, New Astron. 45, 48
Bhattacharyya S. 2010, Adv. Space Res. 45, 949
Boutloukos S., Miller M. C., Lamb F. K. 2010, ApJ, 720, L15
Cominsky L. R., Wood K. S. 1984, ApJ, 283, 765
Díaz Trigo M., Parmar A. N., Boirin L., Méndez M., Kaastra J. S. 2006, A&A, 445, 179
Galloway D. K., Muno M. P., Hartman J. M., Psaltis D., Chakrabarty D., 2008a, ApJS, 179, 360
Galloway D. K., Özel F., Psaltis D. 2008b, MNRAS, 387, 268
Güver T., Özel F. 2013, ApJ, 765, L1
Güver T., Özel F., Psaltis D. 2012a, ApJ, 747, 77
Güver T., Psaltis D., Özel F. 2012b, ApJ, 747, 76
Harrison F. A. *et al*. 2013, ApJ, 770, 103
in't Zand J., Heise J., Smith M. J. S., Cocchi M., Natalucci L., Celidonio G., Augusteijn T., Freyhammer L. 1999, IAU Circ. 7138
Jain C., Paul B., Sharma R., Jaleel A., Dutta A. 2017, MNRAS, 468, L118
Kuulkers E., den Hartog P. R., in't Zand J. J. M., Verbunt F. W. M., Harris W. E., Cocchi M. 2003, A&A, 399, 663
Lewin W. H. G., Hoffman J. A., Doty J., Liller W. 1976, IAU Circ. 2994
Lewin W. H. G., van Paradijs J., Taam R. E. 1993, Space Sci. Rev, 62, 223
Liu Q. Z., van Paradijs J., van den Heuvel E. P. J. 2007, A&A, 469, 807
Muno M. P., Chakrabarty D., Galloway D. K., Savov P. 2001, ApJ, 553, L157
Negoro H. *et al*. 2015, ATel, 7943
Oosterbroek T., Parmar A. N., Sidoli L., in't Zand J. J. M., Heise J. 2001, A&A, 376, 532
Özel F. 2006, Nature, 441, 1115
Parikh A., Wijnands R., Bahramian A., Degenaar N., Heinke C. 2017, ATel, 10169, 169
Sidoli L., Oosterbroek T., Parmar A. N., Lumb D., Erd C. 2001, A&A, 379, 540
Strohmayer T., Bildsten L. 2006, New views of thermonuclear bursts, pp. 113–156
van Paradijs J. 1978, Nature, 274, 650
Wijnands R., Strohmayer T., Franco L. M. 2001, ApJ, 549, L71
Wijnands R., Muno M. P., Miller J. M., Franco L. M., Strohmayer T., Galloway D., Chakrabarty D. 2002, ApJ, 566, 1060
Zhang G., Méndez M., Zamfir M., Cumming A. 2016, MNRAS, 455, 2004